

## Cooperative Catalysis by Tertiary Amino-Thioureas: Mechanism and Basis for Enantioselectivity of Ketone Cyanosilylation

Stephan J. Zuend and Eric N. Jacobsen\*

*Contribution from the Department of Chemistry & Chemical Biology, Harvard University,  
Cambridge, Massachusetts 02138*

Received May 17, 2007; E-mail: jacobsen@chemistry.harvard.edu

**Abstract:** The mechanism of the enantioselective cyanosilylation of ketones catalyzed by tertiary amino-thiourea derivatives was investigated using a combination of experimental and theoretical methods. The kinetic analysis is consistent with a cooperative mechanism in which both the thiourea and the tertiary amine of the catalyst are involved productively in the rate-limiting cyanide addition step. Density functional theory calculations were used to distinguish between mechanisms involving thiourea activation of ketone or of cyanide in the enantioselectivity-determining step. The strong correlation obtained between experimental and calculated ee's for a range of substrates and catalysts provides support for the most favorable calculated transition structures involving amine-bound HCN adding to thiourea-bound ketone. The calculations suggest that enantioselectivity arises from direct interactions between the ketone substrate and the amino-acid derived portion of the catalyst. On the basis of this insight, more enantioselective catalysts with broader substrate scope were prepared and evaluated experimentally.

### Introduction

Cooperative catalysis—the simultaneous binding and activation of two reacting partners—is a fundamental principle in enzymatic catalysis,<sup>1–4</sup> and has emerged as an important strategy in small molecule asymmetric catalysis as well.<sup>5</sup> Indeed, over the past several years, a wide range of synthetically important reactions promoted by chiral small molecules have been identified and proposed to operate by cooperative catalysis.<sup>6</sup> Mechanistic characterization of cooperative enantioselective reactions that involve strong catalyst–substrate interactions (e.g.,

via enamine formation<sup>7</sup> or Lewis acid–Lewis base dative bonding<sup>8,9</sup>) has been possible in several cases. In contrast, mechanistic characterization of catalytic asymmetric reactions involving transient, noncovalent interactions, such as those employed commonly by enzymatic systems, has proved more challenging.<sup>10</sup>

Chiral thioureas represent a versatile and useful class of enantioselective catalysts that function as hydrogen bond donors,<sup>11</sup> and several bifunctional thiourea derivatives have been suggested to operate via cooperative mechanisms.<sup>12</sup> Particularly prominent among these are tertiary amino-thioureas, which have been applied successfully to a wide range of nucleophile–electrophile addition reactions.<sup>13,14</sup> In each case, structure–

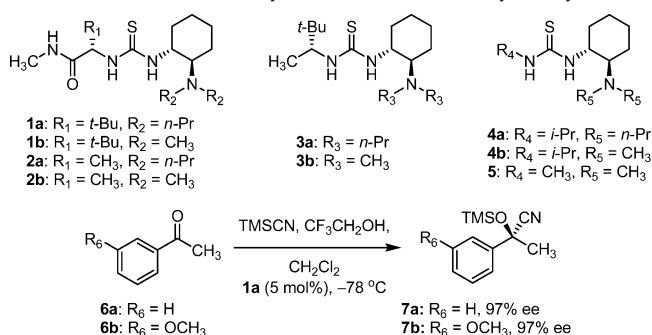
- (1) General discussions: (a) Zeffern, E.; Hall, P. L. *The Study of Enzyme Mechanisms*; Wiley: New York, 1973; Chapter 7. (b) Royer, G. P. *Fundamentals of Enzymology*; Wiley: New York, 1982; Chapter 4. (c) Dugas, H. *Bioorganic Chemistry*; Springer: New York, 1999; Chapter 4. (d) Silverman, R. B. *The Organic Chemistry of Enzyme-Catalyzed Reactions*; Academic Press: San Diego, CA, 2002; Chapter 1. (e) Gerlt, J. A.; Gassman, P. G. *Biochemistry* **1993**, *32*, 11943–11952.
- (2) Selected examples: (a) Breslow, R. *J. Mol. Catal.* **1994**, *91*, 161–174. (b) Zechel, D. L.; Withers, S. G. *Acc. Chem. Res.* **2000**, *33*, 11–18. (c) Hedstrom, L. *Chem. Rev.* **2002**, *102*, 4501–4523. (d) Hopmann, K. H.; Hallberg, B. M.; Himo, F. *J. Am. Chem. Soc.* **2005**, *127*, 14339–14347. (e) Hernick, M.; Gennadios, H. A.; Whittington, D. A.; Rusche, K. M.; Christianson, D. W.; Fierke, C. A. *J. Biol. Chem.* **2005**, *280*, 16969–16978. (f) Cleland, W. W.; Hengge, A. C. *Chem. Rev.* **2006**, *106*, 3252–3278. See, also ref 1d, Chapter 2, 6, and 11.
- (3) Early examples of cooperative mechanisms in small molecules: (a) Swain, C. G.; Brown, J. F. *J. Am. Chem. Soc.* **1952**, *74*, 2534–2537. (b) Swain, C. G.; Brown, J. F. *J. Am. Chem. Soc.* **1952**, *74*, 2538–2543. (c) Morawetz, H.; Oreskes, J. *J. Am. Chem. Soc.* **1958**, *80*, 2591–2592. (d) Kupchan, S. M.; Eriksen, S. P.; Friedman, M. *J. Am. Chem. Soc.* **1966**, *88*, 343–346. (e) Kupchan, S. M.; Eriksen, S. P.; Shen, Y.-T. *J. Am. Chem. Soc.* **1966**, *88*, 347–350. (f) Higuchi, T.; Takechi, H.; Pitman, I. H.; Fung, H. L. *J. Am. Chem. Soc.* **1971**, *93*, 539–540.
- (4) Discussions of concerted general acid-base catalysis: (a) Jencks, W. P. *J. Am. Chem. Soc.* **1972**, *94*, 4731–4732. (b) Jencks, W. P. *Chem. Rev.* **1972**, *72*, 705–718. (c) Gerlt, J. A.; Kozarich, J. W.; Kenyon, G. L.; Gassman, P. G. *J. Am. Chem. Soc.* **1991**, *113*, 9667–9669. (d) Gerlt, J. A.; Gassman, P. G. *J. Am. Chem. Soc.* **1992**, *114*, 5928–5934.
- (5) For a review, see: Ma, J.-A.; Cahard, D. *Angew. Chem., Int. Ed.* **2004**, *43*, 4566–4583.

- (6) (a) Jacobsen, E. N. *Acc. Chem. Res.* **2000**, *33*, 421–431. (b) Shibasaki, M.; Yoshikawa, N. *Chem. Rev.* **2002**, *102*, 2187–2209. (c) Sammis, G. M.; Danjo, H.; Jacobsen, E. N. *J. Am. Chem. Soc.* **2004**, *126*, 9928–9929. (d) Kanai, M.; Kato, N.; Ichikawa, E.; Shibasaki, M. *Synlett* **2005**, *10*, 1491–1508. (e) Shibasaki, M.; Matsunaga, S. *Chem. Soc. Rev.* **2006**, *35*, 269–279.
- (7) For example, as in proline-catalyzed aldol and alkylation reactions: (a) Bahmanyar, S.; Houk, K. N. *J. Am. Chem. Soc.* **2001**, *123*, 12911–12912. (b) Hoang, L.; Bahmanyar, S.; Houk, K. N.; List, B. *J. Am. Chem. Soc.* **2003**, *125*, 16–17. (c) Allemann, C.; Gordillo, R.; Clemente, F. R.; Cheong, P. H.-Y.; Houk, K. N. *Acc. Chem. Res.* **2004**, *37*, 558–569. (d) Fu, A.; List, B.; Thiel, W. *J. Org. Chem.* **2006**, *71*, 320–326. See, also: (e) Yalalov, D. A.; Tsogoeva, S. B.; Schmatz, S. *Adv. Synth. Catal.* **2006**, *348*, 826–832.
- (8) For example, as in the CBS reduction: (a) Corey, E. J.; Azimioara, M.; Sarshar, S. *Tetrahedron Lett.* **1992**, *33*, 3429–3430. (b) Qualllich, G. J.; Blackie, J. F.; Woodall, T. M. *J. Am. Chem. Soc.* **1994**, *116*, 8516–8525. (c) Alagona, G.; Ghio, C.; Persico, M.; Tomasi, S. *J. Am. Chem. Soc.* **2003**, *125*, 10027–10039.
- (9) For example, as in (salen)metal-catalyzed epoxide ring opening: (a) Hansen, K. B.; Leighton, J. L.; Jacobsen, E. N. *J. Am. Chem. Soc.* **1996**, *118*, 10924–10925. (b) Nielsen, L. P. C.; Stevenson, C. P.; Blackmond, D. G.; Jacobsen, E. N. *J. Am. Chem. Soc.* **2004**, *126*, 1360–1362.
- (10) For examples, see: (a) Fearman, M. B.; O'Leary, D. J.; Steinmetz, W. E.; Miller, S. J. *J. Am. Chem. Soc.* **2004**, *126*, 6967–6971. (b) Yamagawa, N.; Qin, H.; Matsunaga, S.; Shibasaki, M. *J. Am. Chem. Soc.* **2005**, *127*, 13419–13427.

activity relationship studies reveal a clear requirement for the tertiary amine, but the respective roles of the thiourea and amine have not been elucidated. Although thiourea activation of the electrophile by hydrogen bonding is often invoked based largely on spectroscopic data of detectable intermediates,<sup>15,16</sup> the well-established anion-binding properties of thioureas<sup>17</sup> raise the possibility that nucleophile binding and activation may be involved instead. Indeed, a detailed theoretical study has shown that the nucleophile-activation mechanism is energetically accessible in some cases, raising questions about the viability of electrophile-activation mechanisms in related reactions.<sup>18</sup> Without a basic understanding of the catalytic mechanism, only speculation about transition structures and the basis for enantioselectivity is possible.

To obtain better insight into the nature and mechanism of cooperative catalysis with thiourea catalysts, we selected the

### Scheme 1. Thiourea-Catalyzed Enantioselective Cyanosilylation



recently discovered ketone cyanosilylation<sup>19,20</sup> promoted by tertiary amino-thiourea catalyst **1a**<sup>13c</sup> as a prototypical reaction for mechanistic analysis (Scheme 1).<sup>21,22</sup> The resulting experimental and theoretical investigation described in this paper has led to the elucidation of a cooperative mechanism, characterization of likely transition structures with insight into the basis for enantioselectivity, and the development of more enantioselective and broadly applicable catalysts.

## Results and Discussion

**A. Kinetic Analysis.** We carried out a detailed kinetic analysis of the ketone cyanation reaction to elucidate the basic composition of the rate-limiting transition structure and identify catalyst resting states.<sup>23</sup> Kinetic studies were performed using representative substrate **6b** and catalyst **1a** at synthetically relevant concentrations using a combination of GC analysis and in situ IR spectroscopy.<sup>24</sup> HCN was generated in situ from TMSCN and CF<sub>3</sub>CH<sub>2</sub>OH,<sup>25</sup> and quantitative formation of HCN

- (11) For reviews, see: (a) Takemoto, Y. *Org. Biomol. Chem.* **2005**, *3*, 4299–4306. (b) Taylor, M. S.; Jacobsen, E. N. *Angew. Chem., Int. Ed.* **2006**, *45*, 1520–1543. (c) Connon, S. J. *Chem. Eur. J.* **2006**, *12*, 5418–5427.
- (12) Primary amino-thioureas: (a) Lalonde, M. P.; Chen, Y.; Jacobsen, E. N. *Angew. Chem., Int. Ed.* **2006**, *45*, 6366–6370 and refs cited therein. Secondary amido-thioureas: (b) Yoon, T. P.; Jacobsen, E. N. *Angew. Chem., Int. Ed.* **2005**, *44*, 466–468. Sulfinamido thioureas: (c) Tan, K. L.; Jacobsen, E. N. *Angew. Chem., Int. Ed.* **2007**, *46*, 1315–1317. Hydroxyl thioureas: (d) Herrera, R. P.; Sgarzani, V.; Bernardi, L.; Ricci, A. *Angew. Chem., Int. Ed.* **2005**, *44*, 6576–6579. Amino-hydroxyl thioureas: (e) Yamaoka, Y.; Miyabe, H.; Takemoto, Y. *J. Am. Chem. Soc.* **2007**, *129*, 6686–6687. Guanidino thioureas: (f) Sohtome, Y.; Hashimoto, Y.; Nagasawa, K. *Adv. Synth. Catal.* **2005**, *347*, 1643–1648.
- (13) Tertiary amino-thiourea catalysts derived from chiral 1,2-diamines: (a) Okino, T.; Hoashi, Y.; Takemoto, Y. *J. Am. Chem. Soc.* **2003**, *125*, 12672–12673. (b) Okino, T.; Hoashi, Y.; Furukawa, T.; Xu, X. N.; Takemoto, Y. *J. Am. Chem. Soc.* **2005**, *127*, 119–125. (c) Fuerst, D. E.; Jacobsen, E. N. *J. Am. Chem. Soc.* **2005**, *127*, 8964–8965. (d) Hoashi, Y.; Okino, T.; Takemoto, Y. *Angew. Chem., Int. Ed.* **2005**, *44*, 4032–4035. (e) Berkessel, A.; Cleemann, F.; Mukherjee, S. *Angew. Chem., Int. Ed.* **2005**, *44*, 7466–7469. (f) Li, H.; Zu, L. S.; Wang, J.; Wang, W. *Tetrahedron Lett.* **2006**, *47*, 3145–3148. (g) Xu, X.; Furukawa, T.; Okino, T.; Miyabe, H.; Takemoto, Y. *Chem. Eur. J.* **2006**, *12*, 466–467. (h) Zu, L. S.; Xie, H. X.; Li, H.; Wang, H.; Jiang, W.; Wang, W. *Adv. Synth. Catal.* **2007**, *349*, 1882–1886.
- (14) Cinchona alkaloid-derived thioureas: (a) Vakulya, B.; Varga, S.; Csampai, A.; Soós, T. *Org. Lett.* **2005**, *7*, 1967–1969. (b) McCooley, S. H.; Connon, S. J. *Angew. Chem., Int. Ed.* **2005**, *44*, 6367–6370. (c) Ye, J. X.; Dixon, D. J.; Hynes, P. S. *Chem. Commun.* **2005**, 4481–4483. (d) Bernardi, L.; Fini, F.; Herrera, R. P.; Ricci, A.; Sgarzani, V. *Tetrahedron* **2006**, *62*, 375–380. (e) Marcelli, T.; van der Haas, R. N. S.; van Maarseveen, J. H.; Hiemstra, H. *Angew. Chem., Int. Ed.* **2006**, *45*, 929–931. (f) Tillman, A. L.; Ye, J. X.; Dixon, D. J. *Chem. Commun.* **2006**, 1191–1193. (g) Mattson, A. E.; Zuhl, A. M.; Reynolds, T. E.; Scheidt, K. A. *J. Am. Chem. Soc.* **2006**, *128*, 4932–4933. (h) Song, J.; Wang, Y.; Deng, L. *J. Am. Chem. Soc.* **2006**, *128*, 6048–6049. (i) Wang, J.; Li, H.; Zu, L. S.; Jiang, W.; Xie, H. X.; Duan, W. H.; Wang, W. *J. Am. Chem. Soc.* **2006**, *128*, 12652–12653. (j) Bode, C. M.; Ting, A.; Schaus, S. E. *Tetrahedron* **2006**, *62*, 11499–11505. (k) Wang, B.; Wu, F.; Wang, Y.; Liu, X. *J. Am. Chem. Soc.* **2007**, *129*, 768–769. (l) Zu, L.; Wang, J.; Li, H.; Hexin, X.; Jiang, W.; Wang, W. *J. Am. Chem. Soc.* **2007**, *129*, 1036–1037. (m) Biddle, M. M.; Lin, M.; Scheidt, K. A. *J. Am. Chem. Soc.* **2007**, *129*, 3830–3831. (n) Wang, Y.; Li, H.; Wang, Q.-W.; Liu, Y.; Foxman, B. M.; Deng, L. *J. Am. Chem. Soc.* **2007**, *129*, 6364–6365. (o) Amere, M.; Lasne, C. M.; Rouden, J. *Org. Lett.* **2007**, *9*, 2621–2624. (p) Liu, T. Y.; Cui, H. L.; Chai, Q.; Long, J.; Li, B. J.; Wu, Y.; Ding, L. S.; Chen, Y. C. *Chem. Commun.* **2007**, 2228–2230. (q) Wang, J.; Zu, L. S.; Li, H.; Xie, H. X.; Wang, W. *Synthesis* **2007**, 2576–2580. (r) Dinér, P.; Nielsen, M.; Bertelsen, S.; Niess, B.; Jørgensen, K. A. *Chem. Commun.* **2007**, 3646–3648. (s) Gu, C. L.; Liu, L.; Sui, Y.; Zhao, J. L.; Wang, D.; Chen, Y. *J. Tetrahedron: Asymmetry* **2007**, *18*, 455–463.
- (15) (a) Vachal, P.; Jacobsen, E. N. *J. Am. Chem. Soc.* **2002**, *124*, 10012–10014. (b) Berkessel, A.; Cleemann, F.; Mukherjee, S.; Müller, T. N.; Lex, J. *Angew. Chem., Int. Ed.* **2005**, *44*, 807–811. (c) Inokuma, T.; Hoashi, Y.; Takemoto, Y. *J. Am. Chem. Soc.* **2006**, *128*, 9413–9419.
- (16) For studies of reactions using achiral thioureas consistent with carbonyl activation, see: (a) Schreiner, P. R.; Wittkopp, A. *Org. Lett.* **2002**, *4*, 217–220. (b) Schreiner, P. R. *Chem. Soc. Rev.* **2003**, *32*, 289–296. (c) Fu, A. P.; Thiel, W. *THEOCHEM* **2006**, *765*, 45–72. (d) Kirsten, M.; Rehbein, J.; Hiersemann, M.; Strassner, T. *J. Org. Chem.* **2007**, *72*, 4001–4011.
- (17) For a review, see: (a) Schmidtchen, F. P.; Berger, M. *Chem. Rev.* **1997**, *97*, 1609–1646. See, also: (b) Antonisse, M. M. G.; Reinholdt, D. N. *Chem. Commun.* **1998**, 443–448. (c) Jagessar, R. C.; Shang, M.; Scheidt, W. R.; Burns, D. H. *J. Am. Chem. Soc.* **1998**, *120*, 11684–11692. (d) Hisaki, I.; Sasaki, S.-I.; Hirose, K.; Tobe, Y. *Eur. J. Org. Chem.* **2007**, 607–615.
- (18) (a) Hamza, A.; Schubert, G.; Soós, T.; Pápai, I. *J. Am. Chem. Soc.* **2006**, *128*, 13151–13160. (b) Rokob, T. A.; Hamza, H. A.; Pápai, I. *Org. Lett.* **2007**, *9*, 4279–4282. See, also: (c) Zhu, Y.; Drueckhammer, D. G. *J. Org. Chem.* **2005**, *70*, 7755–7760. (d) Kotke, M.; Schreiner, P. R. *Synthesis* **2007**, 779–790.
- (19) For other examples of asymmetric ketone cyanosilylation, see: (a) Hamashima, Y.; Kanai, M.; Shibasaki, M. *J. Am. Chem. Soc.* **2000**, *122*, 7412–7413. (b) Tian, S. K.; Deng, L. *J. Am. Chem. Soc.* **2001**, *123*, 6195–6196. (c) Deng, H. B.; Isler, M. R.; Snapper, M. L.; Hoyveda, A. H. *Angew. Chem., Int. Ed.* **2002**, *41*, 1009–1012. (d) Ryu, D. H.; Corey, E. J. *J. Am. Chem. Soc.* **2005**, *127*, 5384–5387. (e) Liu, X. H.; Qin, B.; Zhou, X.; He, B.; Feng, X. M. *J. Am. Chem. Soc.* **2005**, *127*, 12224–12225. (f) Qin, B.; Liu, X. H.; Shi, J.; Zheng, K.; Zhao, H. T.; Feng, X. M. *J. Org. Chem.* **2007**, *72*, 2374–2378 and refs cited therein.
- (20) Reviews: (a) Gregory, R. J. *H. Chem. Rev.* **1999**, *99*, 3649–3682. (b) Brunel, J.-M.; Holmes, I. P. *Angew. Chem., Int. Ed.* **2004**, *43*, 2752–2778.
- (21) Discussions on the biological mechanism for cyanohydrin formation: (a) Wajant, H.; Pfizenmaier, K. *J. Biol. Chem.* **1996**, *271*, 25830–25834. (b) Dreveny, I.; Kratky, C.; Gruber, K. *Protein Sci.* **2002**, *11*, 292–300. (c) Stranzl, G. R.; Gruber, K.; Steinkellner, G.; Zangger, K.; Schwab, H.; Kratky, C. *J. Biol. Chem.* **2004**, *279*, 3699–3707. (d) Gruber, K.; Gartler, G.; Krammer, B.; Schwab, H.; Kratky, C. *J. Biol. Chem.* **2004**, *279*, 20501–20510.
- (22) Mechanistic investigations of the addition of cyanide to carbonyls not promoted by chiral catalysts: (a) Lapworth, A. *J. Chem. Soc.* **1903**, 83, 995–1005. (b) Lapworth, A. *J. Chem. Soc.* **1904**, 85, 1206–1214. (c) Lapworth, A.; Helmuth, R.; Manske, F. *J. Chem. Soc.* **1928**, 2533–2549. (d) Lapworth, A.; Manske, R. H. F. *J. Chem. Soc.* **1930**, 1976–1981. (e) Svrbely, W. J.; Roth, J. F. *J. Am. Chem. Soc.* **1953**, *75*, 3106–3111. (f) Svrbely, W. J.; Brock, F. H. *J. Am. Chem. Soc.* **1955**, *77*, 5789–5792. (g) Ching, W. M.; Kallen, R. G. *J. Am. Chem. Soc.* **1978**, *100*, 6119–6124. (h) Corcoran, R. C.; Ma, J. *J. Am. Chem. Soc.* **1992**, *114*, 4536–4542. (i) Denmark, S. E.; Chung, W.-J. *J. Org. Chem.* **2006**, *71*, 4002–4005.
- (23) Kinetic analyses of catalytic, asymmetric additions of cyanide to C=O or C=N: (a) Takamura, M.; Hamashima, Y.; Usuda, H.; Kanai, M.; Shibasaki, M. *Angew. Chem., Int. Ed.* **2000**, *39*, 1650–1652. (b) Belokon, Y. N.; Green, B.; Ikonnikov, N. S.; Larichev, V. S.; Lokshin, B. V.; Moscalenko, M. A.; North, M.; Orizu, C.; Peregodov, A. S.; Timofeeva, G. I. *Eur. J. Org. Chem.* **2000**, 2655–2661. (c) Josephsohn, N. S.; Kuntz, K. W.; Snapper, M. L.; Hoveyda, A. H. *J. Am. Chem. Soc.* **2001**, *123*, 11594–11599. (d) Belokon, Y. N.; Blacker, A. J.; Carta, P.; Clutterbuck, L. A.; North, M. *Tetrahedron* **2004**, *60*, 10433–10477. (e) Yamagiwa, N.; Tian, J.; Matsunaga, S.; Shibasaki, M. *J. Am. Chem. Soc.* **2005**, *127*, 3413–3422.

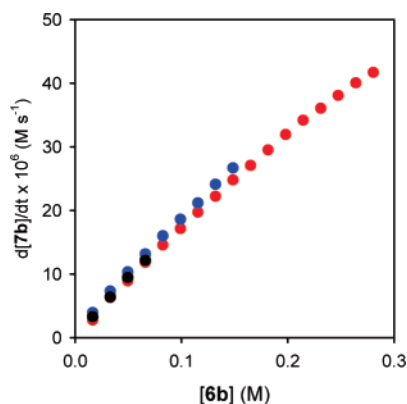


**Figure 1.** Rate dependence on **[6b]**. Plot of the rate of cyanosilylation of **6b** with TMSCN ([TMSCN]<sub>i</sub> = 0.50 M) catalyzed by HCN (0.33 M) and **1a** (0.025 M) at different **[6b]**. Each set of points represents the results from a single in situ IR experiment: (red) **[6b]**<sub>i</sub> = 0.33 M; (blue) **[6b]**<sub>i</sub> = 0.165 M; (black) **[6b]**<sub>i</sub> = 0.083 M.

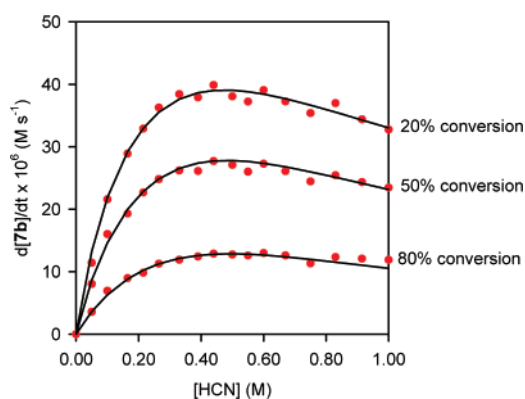


**Figure 2.** Rate dependence on [HCN]. Plot of the rate of cyanosilylation of **6b** (**[6b]**<sub>i</sub> = 0.33 M) with TMSCN ([TMSCN]<sub>i</sub> = 0.50 M) catalyzed by HCN and **1a** (0.025 M) at different [HCN] and at different conversions of **6b**. The curves represent least-squares fits to eq 2; kinetic parameters are given in Scheme 2.

was confirmed by <sup>13</sup>C NMR spectroscopy.<sup>26</sup> The kinetic data revealed the following: (1) Whereas no reaction occurs without HCN, 15 mol % is sufficient to effect >90% substrate conversion. Thus HCN is a cocatalyst for the ketone cyanation. (2) The reaction rate is independent of excess [TMSCN]. (3) Experiments using different initial concentrations of **6b** demonstrated that no appreciable catalyst decomposition or product inhibition occurs over the entire course of the reaction (Figure 2).<sup>24a</sup> (4) Rate inhibition is observed at high [HCN] (Figure 2). (5) The reaction rate displays a less than first-order dependence on **[1a]** at elevated catalyst concentrations (Figure 3). (6) At low concentrations (approximately 0.10 M [HCN], 0.20 M **[6b]**, and 0.015 M **[1a]**), the reaction rate displays a straightforward first-order dependence each on **[1a]**, **[6b]**, and [HCN] (eq 1). These data are consistent with a rate-limiting addition of HCN to **6b** catalyzed by **1a**, followed by a post rate-limiting silylation

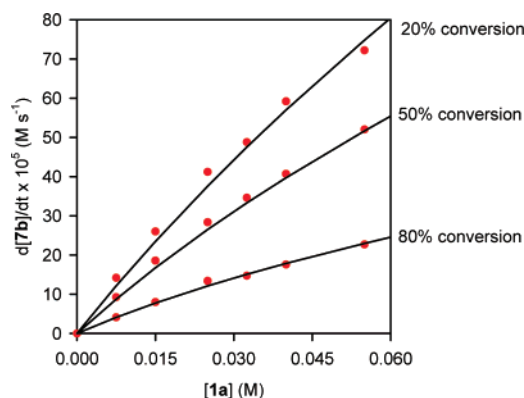
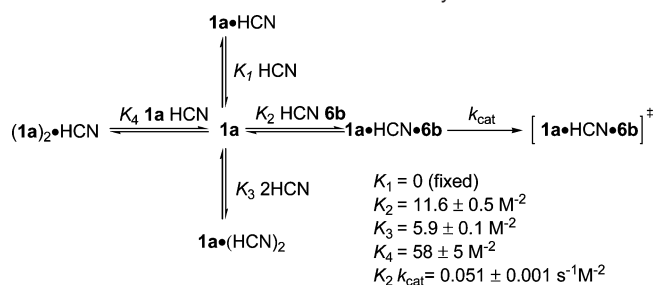


**Figure 3.** Rate dependence on **[1a]**. Plot of the rate of cyanosilylation of **6b** (**[6b]**<sub>i</sub> = 0.33 M) with TMSCN ([TMSCN]<sub>i</sub> = 0.50 M) catalyzed by HCN (0.33 M) and **1a** at different **[1a]** and at different conversions of **6b**. The curves represent least-squares fits to eq 2; kinetic parameters are given in Scheme 2.

#### Scheme 2. Kinetic Parameters for Ketone Cyanation



of an alkoxide or alcohol intermediate to form **7b** and regenerate HCN.

$$\text{rate} = d[7b]/dt = k[1a]^1[6b]^1[HCN]^1[\text{TMSCN}]^0 \quad (1)$$

The deviations from simple first-order kinetic behavior at higher concentrations of catalyst **1a** and HCN point to more complicated and potentially informative nonproductive interactions under certain conditions. To gain insight into these interactions, we used data from 37 individual kinetics experiments to identify an empirical rate law that was valid over a wide range of concentrations.<sup>27</sup> The rate law shown in eq 2 was derived on the basis of the mechanism outlined in Scheme 2,<sup>28</sup> and it is the simplest rate law that provides an adequate fit to the kinetic data (Figures 2 and 3, black curves). The data are consistent with a 1:1:1 complex, **1a**·HCN·**6b**, as the active species. This ternary complex represents the resting state of catalyst only at high **[6b]**. Uncomplexed catalyst is dominant at low concentrations of all species, where the rate law described by eq 2 simplifies to eq 1 (i.e., at low **[6b]** and [HCN] the denominator approaches a value of 1). The observed inhibition at high HCN concentrations is explained through formation of a catalytically inactive 1:2 complex, **1a**·(HCN)<sub>2</sub>. The deviations from integral kinetics in catalyst concentration are explained by a 2:1 complex, (**1a**)<sub>2</sub>·HCN, that becomes dominant at high **[1a]**. All but one of the equilibrium and rate constants could be determined directly from the kinetic data (Scheme 2). Although formation of a 1:1 complex, **1a**·HCN is a likely intermediate step in the formation of the 1:2 complex, **1a**·(HCN)<sub>2</sub>, its

(24) Kinetic analysis of catalytic reactions under synthetically relevant conditions: (a) Blackmond, D. G. *Angew. Chem., Int. Ed.* **2005**, *44*, 4302–4320. (b) Mathew, J. S.; Klussman, M.; Iwamura, H.; Valera, F.; Futran, A.; Emanuelsson, E. A. C.; Blackmond, D. G. *J. Org. Chem.* **2006**, *71*, 4711–4722.

(25) Similar rates and identical enantioselectivities were observed when HCN was generated from CH<sub>3</sub>OH. Addition of independently generated TMSOCH<sub>2</sub>CF<sub>3</sub> had no effect on reaction rate.

(26) Stoichiometric amounts of HCN were generated by adding controlled amounts of CF<sub>3</sub>CH<sub>2</sub>OH to solutions of TMSCN and **1a**. In the absence of **1a**, quantitative formation of HCN from CF<sub>3</sub>CH<sub>2</sub>OH or CH<sub>3</sub>OH and TMSCN in CDCl<sub>3</sub> requires >30 min at room temp; the reaction appears to be nearly instantaneous when **1a** is present.

(27) [HCN] = 0.05–1.00 M; **[7a]** = 0.03–0.26 M; **[1a]** = 0.015–0.055 M; [TMSCN]<sub>i</sub> = 0.50 M. Nonlinear least-squares regression was performed using Sigma Plot version 7.0. Details and kinetic data in tabular format are provided in the Supporting Information.

(28) A derivation of the rate law is provided in the Supporting Information.



$$\text{rate} = \frac{2K_2k_{\text{cat}}[\text{HCN}][\mathbf{6b}][\mathbf{1a}]_{\text{tot}}}{1 + K_1[\text{HCN}] + K_2[\text{HCN}][\mathbf{6b}] + K_3[\text{HCN}]^2 + \sqrt{(1 + K_1[\text{HCN}] + K_2[\text{HCN}][\mathbf{6b}] + K_3[\text{HCN}]^2)^2 + 8K_3[\text{HCN}][\mathbf{1a}]_{\text{tot}}}} \quad (2)$$

formation constant  $K_1$  could not be determined accurately from the kinetic data: values of  $K_1 = 0\text{--}3\text{ M}^{-1}$  all afford good fits to the experimental data and have only a small effect on the other constants (<20% change).<sup>29</sup>

To independently corroborate the individual terms in the rate law and to gain a better understanding of how the thiourea catalyst interacts with and activates HCN and is also susceptible to inhibition, we analyzed the effects of unreactive substrate and catalyst analogues and determined the effect of isotopic substitution of HCN on the reaction rate and enantioselectivity.

**(1) Effect of Added  $\text{CH}_3\text{CN}$  and Pyridine Derivatives.** To determine whether the inhibitory effect observed at high concentrations of HCN may be due to the Lewis basic properties of this substrate, we tested the effect of added  $\text{CH}_3\text{CN}$  on the rate of the thiourea-catalyzed cyanosilylation of ketones (Figure 4). Rate inhibition was observed without any observable change

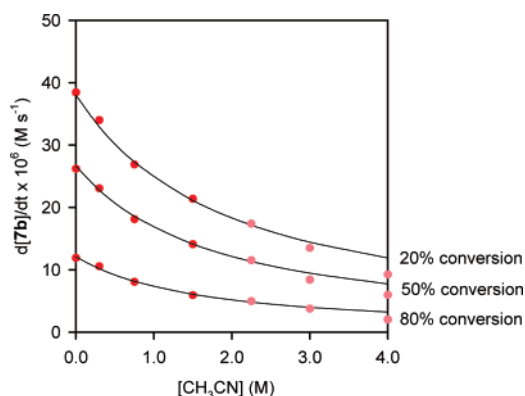


**Figure 4.** Rate dependence on  $[\text{CH}_3\text{CN}]$ . Plot of the rate of cyanosilylation of  $\mathbf{6b}$  ( $[\mathbf{6b}]_i = 0.33\text{ M}$ ) with TMSCN ( $[\text{TMSCN}]_i = 0.50\text{ M}$ ) catalyzed by HCN ( $0.33\text{ M}$ ) and  $\mathbf{1a}$  ( $0.025\text{ M}$ ) in the presence of  $\text{CH}_3\text{CN}$ . The curves represent least-squares fits to eq 3 with  $\text{In} = \text{CH}_3\text{CN}$ ; kinetic parameters are given in Scheme 4. Data from  $[\text{CH}_3\text{CN}] = 0.0\text{--}1.5\text{ M}$  were used in the least-squares fit.

in enantioselectivity (97% ee under all conditions). In principle, this result can be ascribed either to a specific binding interaction or to a general medium effect. Specific interactions are expected to be sensitive to both the electronic and steric properties of the Lewis base, whereas medium effects are expected to be largely insensitive to the steric properties of the Lewis base. We therefore examined the effect of added substituted pyridines on the rate of ketone cyanation (Figure 5).<sup>30</sup> The data reveal that pyridine is a potent inhibitor of ketone cyanosilylation, whereas 2,6-lutidine and 2,6-di-*tert*-butylpyridine are successively weaker inhibitors. In all cases, cyanosilylation product  $\mathbf{7b}$  was isolated in 97% ee. The data provide strong support for a direct interaction between Lewis basic compounds and  $\mathbf{1a}$  rather than a generalized medium effect.

Although catalysis by thiourea derivatives is generally proposed to occur by hydrogen bonding of the thiourea to Lewis basic substrates,<sup>11</sup> direct characterization of such interactions

is not straightforward. Changes in the  $^1\text{H}$  NMR chemical shifts of the thiourea N–H protons have been used to probe these interactions,<sup>13b,15b,31,32</sup> but such experiments cannot always distinguish between direct interactions and medium effects. Indeed, the chemical shifts of all heteroatom-bound protons in thiourea catalysts can change upon addition of Lewis basic substrates.<sup>15a,33</sup> To try to distinguish changes in proton resonances due to specific binding interactions from those due to changes in the medium, we examined the  $^1\text{H}$  NMR chemical shifts of both thiourea protons and the secondary amide proton of  $\mathbf{1a}$  as a function of substituted-pyridine concentration (Figure 6).<sup>34</sup> As expected, the chemical shifts of each of the three  $^1\text{H}$  resonances changed upon titration of each of the three substituted

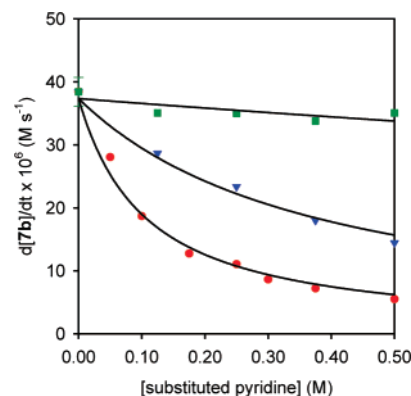


**Figure 5.** Rate dependence on  $[\text{substituted pyridine}]$ . Plot of the rate of cyanosilylation of  $\mathbf{6b}$  ( $[\mathbf{6b}]_i = 0.33\text{ M}$ ) with TMSCN ( $[\text{TMSCN}]_i = 0.50\text{ M}$ ) catalyzed by HCN ( $0.33\text{ M}$ ) and  $\mathbf{1a}$  ( $0.025\text{ M}$ ) in the presence of substituted pyridines: pyridine (●, red), 2,6-lutidine (▼, blue), and 2,6-di-*tert*-butylpyridine (■, green). The curves represent least-squares fits to eq 3;  $\text{In} = \text{pyridine}$ ,  $K_5 = 31 \pm 2\text{ M}^{-1}$ ;  $\text{In} = 2,6\text{-lutidine}$ ,  $K_5 = 8.8 \pm 0.6\text{ M}^{-1}$ ;  $\text{In} = 2,6\text{-di-}t\text{-butylpyridine}$ ,  $K_5 = 0.8 \pm 0.2\text{ M}^{-1}$ .

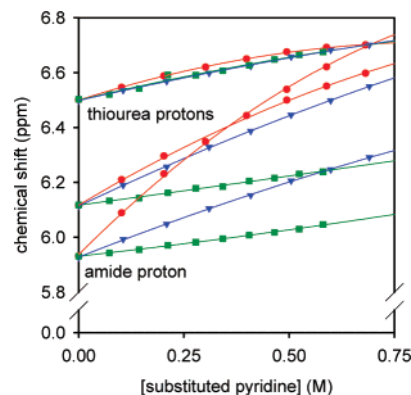


**Figure 6.** Plot of the  $^1\text{H}$  chemical shift of the amide and thiourea protons of  $\mathbf{1a}$  (500 MHz;  $\text{CD}_2\text{Cl}_2$ ;  $[\mathbf{1a}]_i = 0.026\text{ M}$ ,  $22\text{ }^\circ\text{C}$ ) upon titration of various amounts of substituted pyridines as determined by  $^1\text{H}$  NMR spectroscopy. Substituted pyridines: pyridine (●, red), 2,6-lutidine (▼, blue), and 2,6-di-*tert*-butylpyridine (■, green).

(29) If  $K_1$  is unfixed, its value is  $-0.3 \pm 0.2\text{ M}^{-1}$ .

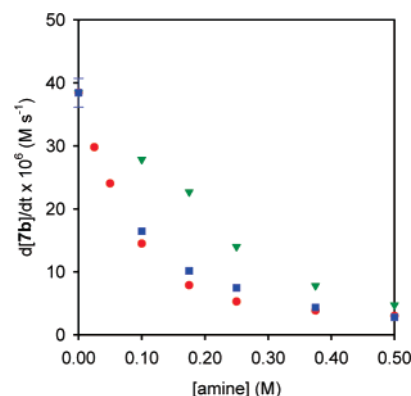
(30) Substituted tetrahydrofuran derivatives have been used in an analogous manner to probe the direct involvement of Lewis basic solvents in reaction mechanisms: (a) Wax, M. J.; Bergman, R. G. *J. Am. Chem. Soc.* **1981**, *103*, 7028–7030. (b) Cotton, J. D.; Markwell, R. D. *Organometallics* **1985**, *4*, 937–939. (c) Galiano-Roth, A. S.; Collum, D. B. *J. Am. Chem. Soc.* **1989**, *111*, 6772–6778. (d) Church, T. L.; Getzler, Y. D. Y. L.; Coates, G. W. *J. Am. Chem. Soc.* **2006**, *128*, 10125–10133.

(31) (a) Kelly, T. R.; Kim, M. H. *J. Am. Chem. Soc.* **1994**, *116*, 7072–7080. (b) Scheerder, J.; Engbersen, J. F. J.; Casnati, A.; Ungaro, R.; Reinhoudt, D. N. *J. Org. Chem.* **1995**, *60*, 6446–6454. (c) Wu, J.-L.; He, Y.-B.; Zeng, Z.-Y.; Wei, L.-H.; Meng, L.-Z.; Yang, T. X. *Tetrahedron* **2004**, *60*, 4309–4314. (d) Brooks, S. J.; Gale, P. A.; Light, M. E. *Chem. Commun.* **2005**, 4696–4698. (e) Brooks, S. J.; Edwards, P. R.; Gale, P. A.; Light, M. E. *New J. Chem.* **2006**, 65–70. (32) For a review, see: Connors, K. A. *Binding Constants*; John Wiley & Sons: New York, 1987. (33) Vachal, P. Ph.D. Thesis, Harvard University, Cambridge, MA, June, 2003.

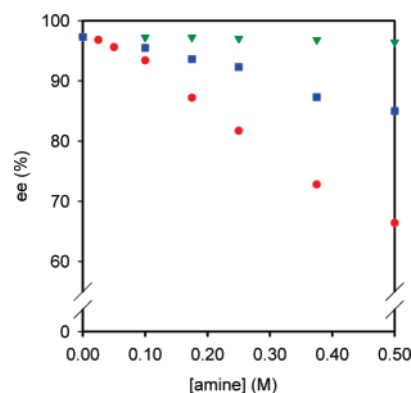
pyridines. However, less sterically demanding pyridines caused significantly greater changes in chemical shift of both the amide and thiourea protons.<sup>35</sup> The fact that the most downfield thiourea proton shows the smallest chemical shift change may be attributed to its internal hydrogen bond to the tertiary amine; DFT calculations suggest that this bond is maintained upon pyridine binding. We attribute these results to a combination of nonspecific, medium effects and specific, pyridine–thiourea interactions that are sensitive to the steric properties of the pyridine derivative.<sup>36</sup>

The kinetic and spectroscopic data demonstrate unambiguously that H-bond acceptors such as pyridine bind to the thiourea of **1a**, and that this binding inhibits the ketone cyanation of **6b** without affecting the enantiomeric excess of the product **7b**. From the similarities in the kinetic behavior of CH<sub>3</sub>CN and pyridine, we infer that CH<sub>3</sub>CN binds to **1a** in an analogous manner under the reaction conditions, and that HCN also binds to the thiourea moiety of **1a** through its Lewis basic nitrogen lone pair. The observation of constant enantioselectivity in the presence or absence of CH<sub>3</sub>CN suggests that the mechanism of the productive pathway remains unchanged; that is, no reaction occurs when the inhibitor is bound to the catalyst, because such a mechanism would almost certainly induce different enantioselectivity. It can be concluded that the thiourea functionality is involved directly in catalysis of cyanosilylation; however, the data do not reveal how the thiourea is involved in the catalytic mechanism. Thus, although we conclude that HCN can bind to the thiourea as a Lewis base, we cannot determine whether this binding is productive (i.e., on the catalytic cycle) or inhibitory (off the catalytic cycle): inferring a transition structure from an observable substrate–catalyst interaction could lead to invalid conclusions.<sup>37</sup>

**(2) Effect of Added Trialkylamines.** To establish whether the trialkylamine portion of **1a** is involved in either productive



**Figure 7.** Rate dependence on [trialkylamine]. Plot of the rate of cyanosilylation of **6b** ( $[\mathbf{6b}]_i = 0.33$  M) with TMSCN ( $[\text{TMSCN}]_i = 0.50$  M) catalyzed by HCN (0.33 M) and **1a** (0.025 M) in the presence of trialkylamines: *i*-Pr<sub>2</sub>NEt (●, red), Et<sub>3</sub>N (■, blue), and Me<sub>2</sub>NEt (▼, green). Rate data were obtained at 20% conversion of **6b**.

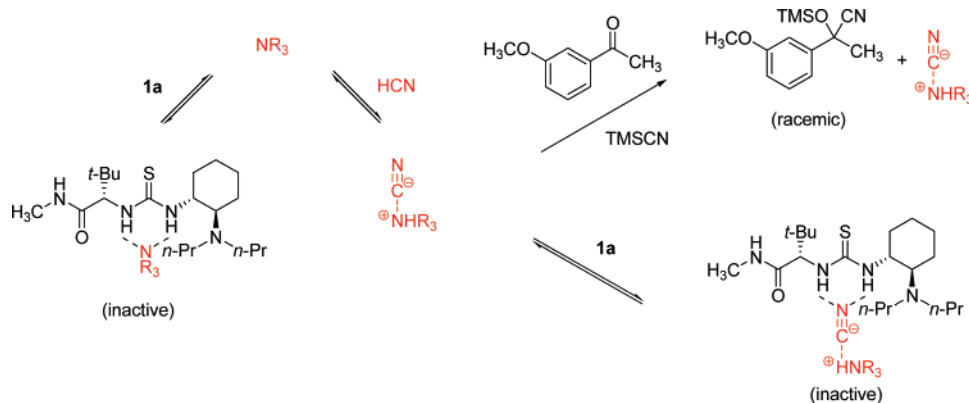


**Figure 8.** Effect of trialkylamines on enantioselectivity. Plot of the enantiomeric excess (%) of **7b** obtained in the cyanosilylation of **6b** ( $[\mathbf{6b}]_i = 0.33$  M) with TMSCN catalyzed by HCN (0.33 M) and **1a** (0.025 M) in the presence of trialkylamines: *i*-Pr<sub>2</sub>NEt (●, red), Et<sub>3</sub>N (■, blue), and Me<sub>2</sub>NEt (▼, green).

- (34) The <sup>1</sup>H NMR spectrum of **1a** becomes uninterpretable below ca. −10 °C, presumably because bond rotation occurs on NMR time scales at those temperatures. We were thus limited to NMR experiments at or near room temperature.
- (35) The binding constants of pyridine and substituted pyridines with different metal ions have been determined: Kapinos, L. E.; Sigel, H. *Inorg. Chim. Acta* **2002**, *337*, 131–142.
- (36) The correlation between the steric properties of the Lewis base and the binding affinity to the thiourea might suggest that catalysts such as **1a** and **1b** might be highly sensitive to substrate structure and therefore limited in scope. However, this is not the case in the ketone cyanation reaction. Despite compelling evidence that cyanosilylation proceeds via ketone binding to the thiourea protons (vide infra), the reaction rate and enantioselectivity are remarkably insensitive to the steric properties of the ketone. <sup>1</sup>H NMR studies of acetophenone derivatives with differing steric properties (acetophenone, isobutyrophenone, and 2,2-dimethylpropylphenone) also revealed relatively small chemical shift changes (0.1–0.3 ppm) that were insensitive to the steric properties of the substrate. These observations may be ascribed simply to the fact that the ketone substituents are remote from the catalyst compared to the substituents on 2,6-disubstituted pyridines.
- (37) For the classic example in the context of asymmetric catalysis, see: Halpern, J. *Science* **1982**, *217*, 401–407.
- (38) For a compilation of the gas-phase basicities (proton affinities) of sterically differentiated amines, see: Drago, R. S.; Cundari, T. R.; Ferris, D. C. *J. Org. Chem.* **1989**, *54*, 1042–1047. Proton affinity is strongly correlated with the number and size of alkyl groups on the amine. For example, PA(NH<sub>3</sub>) = 204.0, PA(NMe<sub>3</sub>) = 225.1, PA(NEt<sub>3</sub>) = 232.3.
- (39) *n*-Bu<sub>4</sub>CN was also found to be a potent inhibitor of ketone cyanosilylation. Unfortunately, we were unable to achieve conditions under which kinetic data with this inhibitor were reproducible, perhaps because of the hygroscopic nature of this reagent.
- (40) In the absence of **1a**, *i*-Pr<sub>2</sub>NEt mediates the cyanosilylation of **6b** at a rate sufficient to account for the reduced ee observed under the catalytic conditions (4% conversion after 4 h with 0.50 M *i*-Pr<sub>2</sub>NEt). In contrast, Me<sub>2</sub>NEt does not mediate the cyanosilylation of **6b** at −78 °C (< 0.5% conversion after 4 h with 0.50 M Me<sub>2</sub>NEt).
- (41)  $K_2 = 20 \pm 1$  M<sup>−2</sup>,  $K_3 = 25 \pm 1$  M<sup>−2</sup>,  $K_4 = 96 \pm 30$  M<sup>−2</sup>,  $K_2k_{\text{cat}} = 0.099 \pm 0.005$  s<sup>−1</sup> M<sup>−2</sup>. As with HCN, an accurate value for  $K_1$  could not be determined, and  $K_1 = 0$  was used for the analysis.

or unproductive interactions with HCN, we examined the effect of exogenous trialkylamines (dimethylethylamine, Me<sub>2</sub>NEt; triethylamine, Et<sub>3</sub>N; diisopropylethylamine, *i*-Pr<sub>2</sub>NEt) on the rate and enantioselectivity of ketone cyanosilylation (Figures 7 and 8). The data reveal that the degree of rate inhibition and the observed decreases in enantioselectivity correlate with the size of the trialkylamine. It is possible that trialkylamines bind to the thiourea of **1a** directly. However, titration of **1a** with trialkylamines revealed the same dependence on steric properties as observed with substituted pyridines. Addition of up to 0.50 M *i*-Pr<sub>2</sub>NEt to a 0.026 M solution of **1a** in CD<sub>2</sub>Cl<sub>2</sub> resulted in no significant changes to the chemical shifts of either the amide or thiourea protons (<0.05 ppm); addition of Et<sub>3</sub>N and Me<sub>2</sub>NEt resulted in small but significant changes (up to 0.2 and 0.5 ppm, respectively). Because the inhibition trends determined kinetically and the binding trends determined spectroscopically show opposite dependence on the steric properties of trialkylamines, we conclude that direct binding cannot be solely responsible for rate inhibition. Instead, the inhibition effects may be explained by the fact that the Brønsted basicity of trialkylamines also correlates with their size.<sup>38</sup> It is likely that

- (42) Details are provided in the Supporting Information. Because the inhibition effect by DCN is greater than with HCN, this KIE represents an upper limit for the intrinsic KIE (i.e., the true intrinsic KIE,  $k_H/k_D$ , is  $\leq 0.64 \pm 0.04$ ). Although it is possible, in principle, to determine the KIE more accurately from experiments at lower concentrations of HCN and DCN, such experiments are prone to both random and systematic error because trace amounts of water can generate HCN from TMSCN.

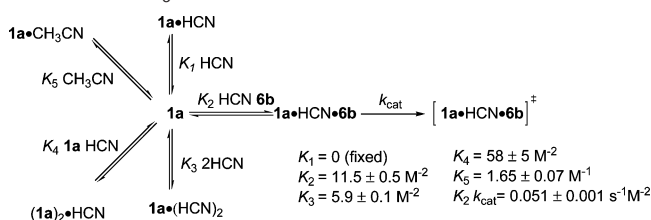
**Scheme 3.** Possible Modes of Rate Inhibition and Enantioselectivity Suppression Induced by Trialkylamines

trialkylamines engage in a hydrogen-bond interaction with HCN under the reaction conditions, and the resulting complex may inhibit cyanosilylation by binding to **1a**, in a manner analogous to the much weaker binding of neutral HCN or CH<sub>3</sub>CN (Scheme 3).<sup>39</sup> Trialkylamines also catalyze a racemic reaction, leading to depressed ee's at high concentrations, and more basic trialkylamines promote such pathways more effectively.<sup>40</sup> The trends that are observed with exogenous trialkylamines are also pronounced with tertiary amino-thiourea catalysts: di-*n*-propylamino catalyst **1a** catalyzes the cyanosilylation of **6b** 20 times faster than dimethylamino **1b**, and with slightly higher enantiomeric excess (97% ee versus 95% ee).

**(3) Isotope Effects: Comparison of HCN and DCN.** The rates of both HCN- and DCN-promoted ketone cyanosilylation were measured over a 20-fold range of [HCN] and [DCN] (Figure 9). Kinetic modeling over the entire range of DCN concentrations reveals excellent agreement with the rate law given by eq 2 and demonstrates that both the intrinsic rate (at low concentrations) and the inhibitory effect (at high concentrations) are greater with DCN than with HCN.<sup>41</sup> Comparison of the rates at low concentrations of HCN and DCN where the inhibitory effect is small ( $\leq 0.10$  M) allows us to estimate an intrinsic kinetic isotope effect ( $k_H/k_D$ ) of  $0.64 \pm 0.05$ .<sup>42</sup> Both effects may be associated with the greater acidity of DCN if its partial or complete deprotonation plays a role in both the productive and inhibitory pathways. Although a priori predictions of relative acidities of isotopically labeled compounds can be challenging and depend on the degree of proton transfer,<sup>43</sup> a

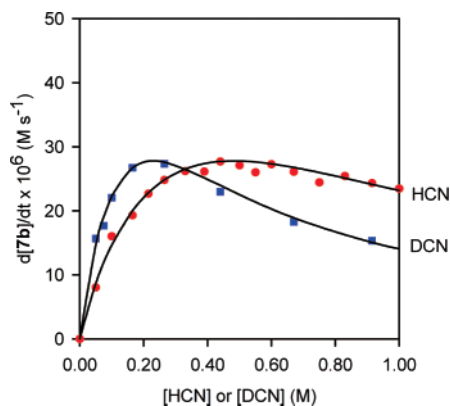
slightly stronger hydrogen bond has been observed in the gas phase between DCN and NMe<sub>3</sub> than between HCN and NMe<sub>3</sub>.<sup>44,45</sup> The greater acidity of DCN in this reaction is also borne out by DFT calculations described below.<sup>46</sup>

**B. Mechanistic Possibilities.** The kinetic analysis using Lewis and Brønsted basic additives has revealed several modes of inhibition, as predicted by eq 2. To test whether the effects of exogenous inhibitors could themselves be modeled quantitatively, we derived an analogous rate law that accounts for direct inhibition via hydrogen bonding to **1a** (eq 3, Scheme 4).

**Scheme 4.** Kinetic Parameters for Ketone Cyanation in the Presence of CH<sub>3</sub>CN

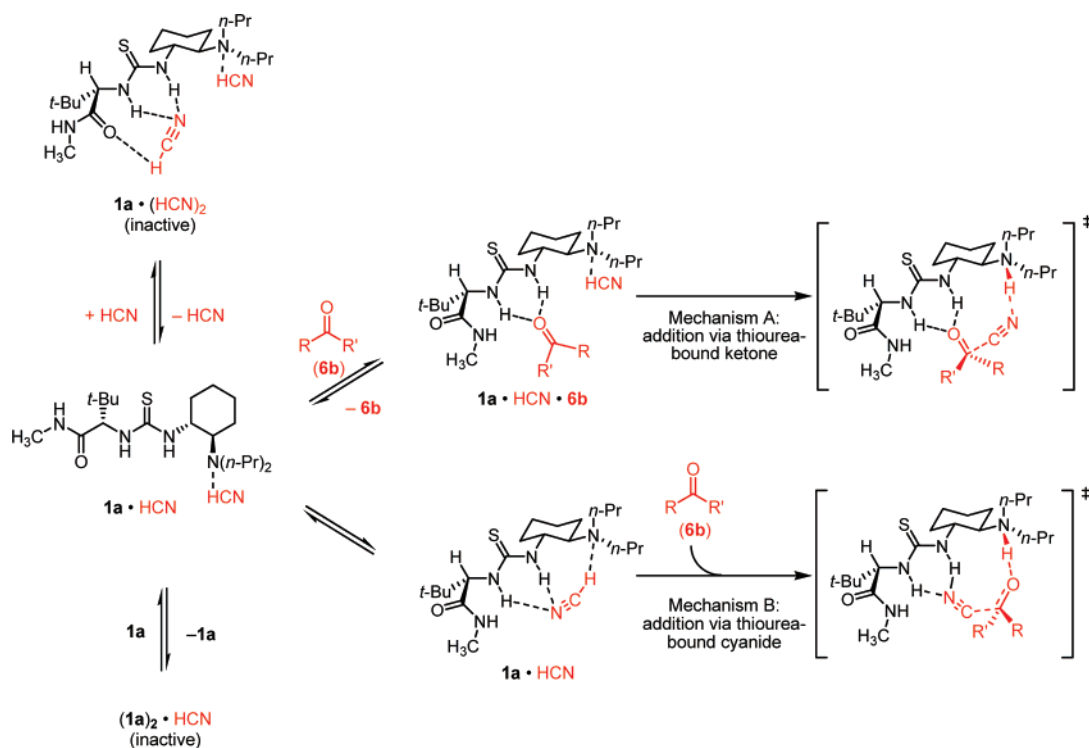
Rate data in the presence of inhibitors most structurally analogous to HCN and **1a** were used at concentrations similar to those in the catalytic reaction (e.g., [CH<sub>3</sub>CN] = 0.3–1.5 M). Lewis basic pyridine derivatives were shown to bind to the thiourea of **1a**, and both CH<sub>3</sub>CN and HCN appear to be sufficiently basic to do so as well. Thus the binding constant of CH<sub>3</sub>CN ( $K_5 = 1.65 \pm 0.07$  M<sup>-1</sup>) provides an estimate for the binding constant of HCN as a Lewis base (Scheme 4). The binding constants of substituted pyridines were determined in an analogous manner (Figure 5).

It is striking that the factors that contribute to effective catalysis are the same factors that lead to depressed rates at



**Figure 9.** Rate dependence on [HCN] and [DCN]. Plot of the rate of cyanosilylation of **6b** ([**6b**]<sub>i</sub> = 0.33 M) with TMSCN ([TMSCN]<sub>i</sub> = 0.50 M) catalyzed by HCN and **1a** (0.025 M) at different [HCN] or [DCN] at 50% conversion of **6b**. The curves represent least-squares fits to eq 2.

- (43) (a) Scheiner, S.; Èuma, M. *J. Am. Chem. Soc.* **1996**, *118*, 1511–1521. (b) Scheiner, S. *Hydrogen Bonding: A Theoretical Perspective*, Oxford University Press: New York, 1997. (c) Scheiner, S. *Biochem. Biophys. Acta* **2000**, 28–42.
- (44) Rego, C. A.; Batten, R. C.; Legon, A. C. *J. Chem. Phys.* **1998**, *89*, 696–702.
- (45) HCN/DCN isotope effects: (a) Hout, R. F., Jr.; Wolfsberg, M.; Hehre, W. *J. Am. Chem. Soc.* **1980**, *102*, 3296–3298. (b) Reenstra, W. W.; Abeles, R. H.; Jencks, W. P. *J. Am. Chem. Soc.* **1982**, *104*, 1016–1024. (c) Cybulski, S. M.; Scheiner, S. *J. Am. Chem. Soc.* **1987**, *109*, 4199–4206. (d) Zabarnick, S.; Fleming, J. W.; Lin, M. C. *Chem. Phys.* **1991**, *150*, 109–115. (e) McDowell, S. A. C.; Forde, T. S. *J. Chem. Phys.* **2002**, *117*, 6032–6037. See also ref 33.
- (46) It is interesting that the complex kinetic dependence on HCN (1st order at low concentrations, negative order at high concentrations) leads to a situation where there is almost no KIE at the concentrations at which the reaction is normally run (0.30–0.40 M).

Scheme 5. Mechanistic Possibilities<sup>a</sup>

<sup>a</sup> Both mechanisms are consistent with the experimentally determined rate law and are kinetically indistinguishable. The structures of these intermediates are based on DFT calculations (B3LYP/6-31G(d)) using model catalyst **1b**.

$$\text{rate} = \frac{2K_2 k_{\text{cat}} [\text{HCN}][\mathbf{6b}][\mathbf{1a}]_{\text{tot}}}{1 + K_1[\text{HCN}] + K_2[\text{HCN}][\mathbf{6b}] + K_3[\text{HCN}]^2 + K_5[\text{In}] + \sqrt{(1 + K_1[\text{HCN}] + K_2[\text{HCN}][\mathbf{6b}] + K_3[\text{HCN}]^2 + K_5[\text{In}])^2 + 8K_3[\text{HCN}][\mathbf{1a}]_{\text{tot}}}} \quad (3)$$

high concentrations: (1) more basic amines are both better catalysts (**1a** versus **1b**) and stronger inhibitors (*i*-Pr<sub>2</sub>NEt versus Me<sub>2</sub>NEt) and (2) DCN is both more reactive at low concentrations and a better inhibitor at high concentrations than HCN. Scheme 5 depicts a plausible set of equilibria that accounts for the observations gleaned from the kinetic analysis.<sup>47</sup> One mode of catalyst inhibition at high concentrations of HCN is via formation of a 1:2 complex between **1a** and HCN (**1a**•2HCN, Scheme 5). In addition, trialkylamines including **1a** are basic enough to complex or deprotonate HCN and DCN, and general or specific base activation of HCN/DCN is important for both catalysis and inhibition. Inhibition by trialkylamines likely occurs through the formation of cyanide anion, which is more Lewis basic than HCN and so binds to thioureas at lower concentrations. The lower-than-first-order kinetic dependence on **1a** may be ascribed to the reversible formation of inactive catalyst aggregates, either spontaneously or through bridging cyanide ions. The latter possibility is supported by the observed inhibitory effect of simple tertiary amine additives.<sup>48</sup>

The key findings of the kinetic analysis—that tertiary amine activation of HCN is important for catalysis and unproductive binding to the thiourea of **1a** inhibits catalysis—provide compelling evidence that both the thiourea and the trialkylamine functions of **1a** are involved directly in the catalytic pathway.

However the kinetic analysis also demonstrates that multiple modes exist for catalyst association to HCN, and the data do not allow us to distinguish productive and unproductive binding modes. Two mechanisms that are consistent with the available data are depicted in Scheme 5: mechanism A involves addition of cyanide to a thiourea-bound ketone, whereas mechanism B involves addition of thiourea-bound cyanide to a ketone activated by the protonated amine. Because the species depicted in Scheme 5 are in rapid equilibrium,<sup>49</sup> a kinetic analysis alone cannot distinguish between these mechanisms: both have transition structures with identical compositions and both involve HCN deprotonation, and therefore have identical elementary rate laws and similar predicted isotope effects. Assessing which of these mechanisms is operative therefore requires an alternative approach.

**C. Theoretical Analysis of the Selectivity-Determining Step.** Despite the complexities observed in the kinetic analysis, the enantioselectivity of ketone cyanosilylation is unchanged over a range of concentrations. The lack of dependence of enantioselectivity on reaction conditions suggests that the transition structures leading to the major and minor enantiomer have the same stoichiometry, and the selectivity-determining

(47) The structures of these intermediates are based on DFT calculations (B3LYP/6-31G(d)) using model catalyst **1b**. The calculations suggest that the secondary amide lone pair may play a role in HCN binding, perhaps providing an explanation for the large inhibitory effect observed kinetically. However, evaluating the importance of such an interaction will require higher level calculations and inclusion of solvent effects.

(48) <sup>1</sup>H NMR experiments show that the chemical shifts of the amide and thiourea protons of **1a** are concentration-dependent in the absence of other substrates; however, the addition of 2,6-di-*tert*-butylpyridine results in small but significant <sup>1</sup>H NMR chemical shift changes without inhibiting the rate of ketone cyanosilylation. Thus a concentration-dependent <sup>1</sup>H NMR spectrum does not constitute evidence for catalyst aggregation. IR spectra of **1a** (0.02–0.10 M) show good adherence to Beer's law, indicating that significant direct aggregation does not occur. The possibility of small amounts of direct aggregation cannot be excluded, but this would not change our overall conclusions. Details are included in the Supporting Information.



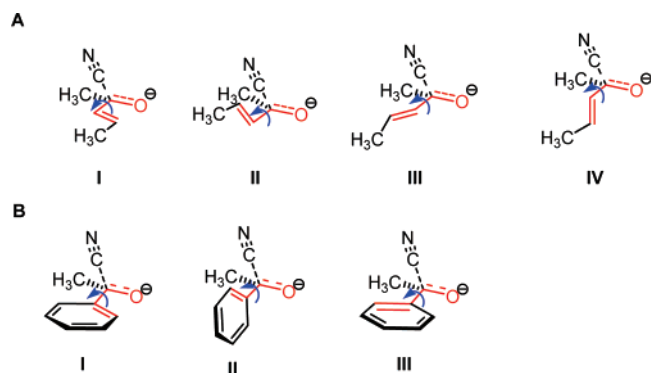


**Figure 10.** Variation of C–C–C–O dihedral angles between C=O and C=C (shown in red) in the transition structures for cyanide ion addition to (A) 3-penten-2-one and (B) acetophenone in the absence of catalyst.

step is the same under all conditions examined. Encouraged that this system is mechanistically well behaved and therefore may be amenable to theoretical analysis, we turned to density functional theory (DFT) calculations to distinguish between the pathways involving HCN–amine interactions depicted in Scheme 5.<sup>50,51</sup> Although DFT methods have been used successfully to probe the mechanisms of catalytic asymmetric reactions, limitations have also been noted;<sup>52</sup> however, the wealth of available enantioselectivity data in the ketone cyanation reaction might allow correlation between experiment and theory and serve to validate the computational results.

Our analysis began with a thorough conformational study of **1b**, which catalyzes the cyanosilylation of acetophenone (**6a**) with 95% ee, using the B3LYP level of theory<sup>53</sup> and several basis sets.<sup>54</sup> We then examined the transition structure for the gas-phase addition of anionic cyanide to 3-penten-2-one and acetophenone in the absence of catalyst (Figure 10). In both cases, transition structures were identified in which the C=O bond was nearly coplanar with the C=C bond (in 3-penten-2-one) or the aromatic ring (in acetophenone). The energetic cost of accessing conformations in which these bonds were not coplanar was assessed by systematically varying the C–C–C–O dihedral angle between the C=O and C=C bonds for the transition structures shown in Figure 10.<sup>55</sup> The data reveal a distinct preference of the C=O of the electrophile to be coplanar with the C=C bond in the transition structure for both substrates (Figure 11). Two minimum energy conformations were identified for 3-penten-2-one (A, *s*-cis, **I**; and a distorted *s*-trans, **III**), but the *s*-cis transition structure is significantly more stable; because of its rotational symmetry, acetophenone has only one minimum energy conformation (i.e., B, **I** = **III**).

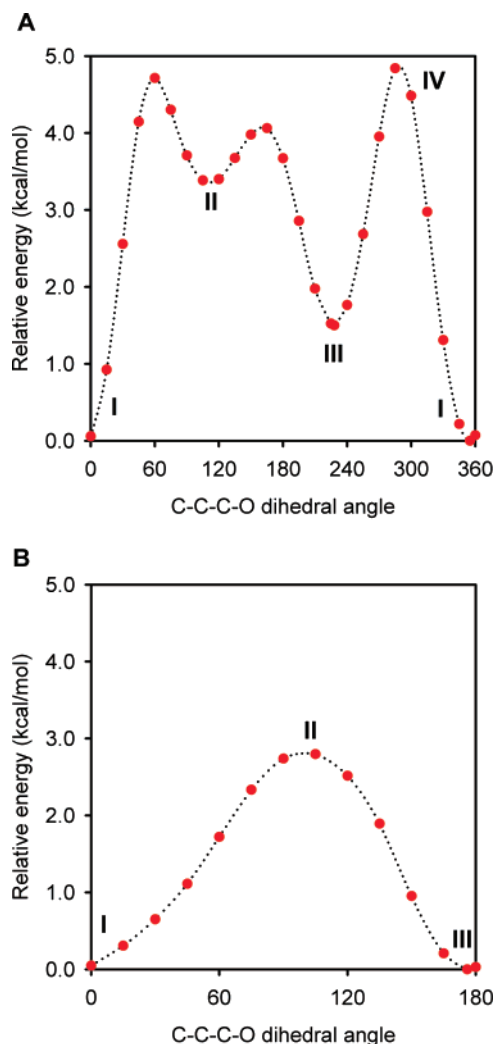


**Figure 11.** Torsional energy profiles for the addition of cyanide ion to (A) 3-penten-2-one and (B) acetophenone. Plot of relative energy of cyanide addition transition structure at the B3LYP/6-31+G(d,p) level versus C–C–C–O dihedral angle. Selected structures are depicted in Figure 10.

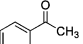
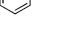
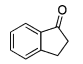
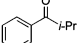
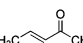
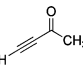
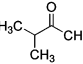
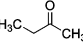
Transition-state calculations at the B3LYP/6-31G(d) level<sup>56,57</sup> on the cyanide addition to acetophenone promoted by amino-thiourea catalysts reveal geometries that are remarkably similar to the calculated transition-structure geometries in the absence of catalyst (Supporting Information). Most significant, calculations on model catalyst **5** indicate that both mechanisms A and

- (49) <sup>1</sup>H NMR spectra reveal only two thiourea resonances under all conditions examined, consistent with rapid exchange. Unlike most other carbon acids, HCN undergoes rapid proton exchange with oxygen and nitrogen bases: (a) Bednar, P. A.; Jencks, W. P. *J. Am. Chem. Soc.* **1985**, *107*, 7117–7126. (b) Bednar, P. A.; Jencks, W. P. *J. Am. Chem. Soc.* **1985**, *107*, 7126–7134.
- (50) DFT calculations were carried out using Gaussian 98 or Gaussian 03: Frisch, M. J.; et al. *Gaussian 03*; Gaussian, Inc.: Pittsburgh, PA, 2003.
- (51) For theoretical studies on the addition of cyanide to imines, see: (a) Arnaud, R.; Adamo, C.; Cossi, M.; Milet, A.; Vallée, Y.; Barone, V. *J. Am. Chem. Soc.* **2000**, *122*, 324–330. (b) Li, J.; Jiang, W.-Y.; Han, K. L.; He, G.-Z.; Li, C. *J. Org. Chem.* **2003**, *68*, 8786–8789. (c) Su, Z. S.; Hu, C. W.; Qin, S.; Feng, X. M. *Tetrahedron* **2006**, *62*, 4071–4080.
- (52) Wodrich, M. D.; Corninboeuf, C.; Schreiner, P. R.; Fokin, A. A.; Shleyer, P. v. R. *Org. Lett.* **2007**, *9*, 1851–1854.
- (53) (a) Lee, C.; Yang, W.; Parr, R. G. *Phys. Rev. B* **1988**, *37*, 785–789. (b) Becke, A. D. *J. Chem. Phys.* **1993**, *98*, 1372–1377.
- (54) Details of these analyses are provided in the Supporting Information.

- (55) Conformational analysis was performed by first locating the lowest energy transition structure for the addition of cyanide to each substrate. The length of partially formed C–C bond between cyanide and the carbonyl was found to be 2.030 Å for acetophenone and 1.945 Å for 3-penten-2-one. This C–C bond distance was then fixed, and the C–C–C–O dihedral (shown in red) was varied in 15° increments. A geometry optimization was performed at each point with all other coordinates fully relaxed. The transition structures in which the C–C–C–O dihedral angle is varied will likely have somewhat different optimal C–C bond lengths in the true transition structures for those conformations, so this procedure provides a lower limit for the energetic preference for the aromatic ring or vinyl group and the reacting C=O bond to be coplanar in the transition structure.
- (56) Calculations at the B3LYP level of theory using the 6–31G(d) basis set have been shown previously to reproduce relative energies of diastereomeric transition states that involve hydrogen bonding or hydrogen atom transfer. For examples, see: (a) Bahmanyar, S.; Houk, K. N.; Martin, H. J.; List, B. *J. Am. Chem. Soc.* **2003**, *125*, 2475–2479. (b) Bahmanyar, S.; Houk, K. N. *Org. Lett.* **2003**, *5*, 1249–1251. (c) Cheong, P. H.-Y.; Houk, K. *J. Am. Chem. Soc.* **2004**, *126*, 13912–13913.
- (57) For a discussion on differences between the 6-31G(d) and 6-31+G(d,p) basis sets in catalytic asymmetric reactions involving hydrogen atom transfer see: Clemente, F. R.; Houk, K. N. *J. Am. Chem. Soc.* **2005**, *127*, 11294–11302.



**Table 1.** Experimental and Calculated Relative Activation Energies for the Cyanosilylation of Ketones<sup>a</sup>

entry	ketone	catalyst <sup>b</sup>	exp. ee(%)	exp. $\Delta\Delta G^\ddagger$ (kcal/mol)	calc. $\Delta\Delta E^\ddagger$ (kcal/mol)
1		<b>1a</b>	97	1.6	2.7 (2.7)
2		<b>2a</b>	90	1.1	1.8 (1.6)
3		<b>3a</b>	90	1.1	2.0 (1.6)
4		<b>4a</b>	79	0.8	0.9 (1.3)
5		<b>1a</b>	91	1.2	1.2 (1.8)
6		<b>1a</b>	86	1.0	2.1 (2.4)
7		<b>1a</b>	89	1.1	2.2 <sup>c</sup> (1.7)
8		<b>1a</b>	63	0.6	1.4 (1.1)
9		<b>1a</b>	19	0.2	0.4 (0.1)
10		<b>1a</b>	11	0.1	0.3 (0.1)

<sup>a</sup> Experimental ee's were determined by chiral GC from reactions run on 0.2 mmol scale at  $-78^\circ\text{C}$  using 2.2 equiv TMSCN, 1.0 equiv  $\text{F}_3\text{CCH}_2\text{OH}$ , and 5–10 mol % catalyst in  $\text{CH}_2\text{Cl}_2$  (0.4 M).  $\Delta\Delta G^\ddagger$  values were estimated with:  $\Delta\Delta G^\ddagger = -RT \ln(k_S/k_R)$ ,  $T = 195\text{ K}$ . Calculated  $\Delta\Delta E^\ddagger$  values were determined using the B3LYP/6-31G(d) level of density functional theory and include a zero-point energy correction scaled by 0.9806 (Scott, A. P.; Radom, L. *J. Phys. Chem.* **1996**, *100*, 16502–16513). Transition structures were fully optimized and shown to have a single imaginary frequency. Values in parentheses are derived from single-point energy calculations at the mPW1K/6-31+G(d,p)//B3LYP/6-31G(d) level. <sup>b</sup> Experimental selectivities were determined using the dipropylamine catalysts listed; calculations were conducted with their dimethylamine analogues (i.e., **1b**, **2b**, **3b**, and **4b**). <sup>c</sup> Four transition structures were located with the following relative energies (kcal/mol): *S*, *s*-cis: 0.0; *R*, *s*-cis: 2.2 (1.7); *S*, *s*-trans: 2.8 (2.3); *R*, *s*-trans: 2.9 (2.4).

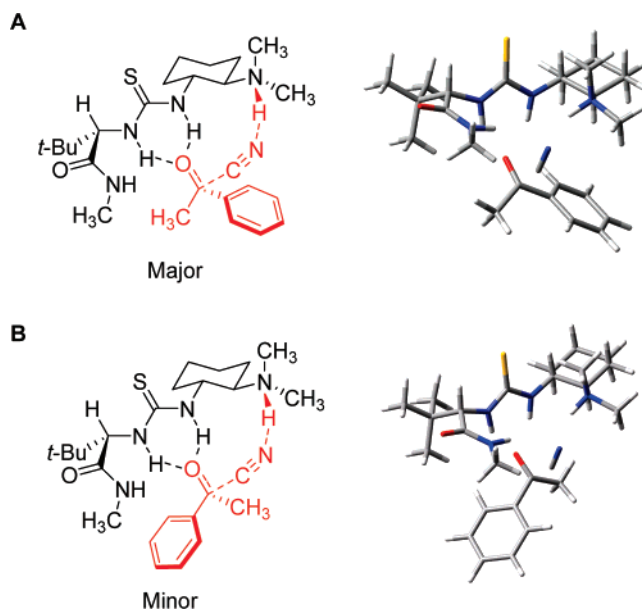
B in Scheme 5 are energetically accessible, but that mechanism A is significantly (major enantiomer: 4.7 kcal/mol) more favorable. Furthermore, calculations of diastereomeric transition states within mechanism A using catalyst **1b** predict the experimentally observed enantiomer of product ( $\Delta\Delta E^\ddagger = 0.9$  kcal/mol); analogous calculations within mechanism B identify no basis for enantioselectivity ( $\Delta\Delta E^\ddagger = 0.0$  kcal/mol).<sup>58</sup> All transition structures were shown to be legitimate first-order saddle points by the existence of a single imaginary frequency corresponding to the addition of cyanide to the C=O bond.

Transition state calculations at the B3LYP/6-31G(d) level of several substrate–catalyst combinations undergoing reaction by mechanism A reveal solid agreement with experimental trends (Table 1). Nearly identical trends were observed with single-point energy calculations at the mPW1K/6-31+G(d,p) level.<sup>59–62</sup>

(58) Larger basis sets (6-31G(d,p) and 6-31+G(d,p)) afford no significant change in relative energy ( $<0.3$  kcal/mol) or geometry for a model system (see Supporting Information for details). In addition, single-point calculations at the mPW1K/6-31+G(d,p)//B3LYP/6-31G(d) level provide similar results: thiourea–ketone, *S* = 0.0 kcal/mol, *R* = 0.9 kcal/mol; thiourea–cyanide, *S* = 4.5 kcal/mol, *R* = 4.9 kcal/mol.

(59) Lynch, B. J.; Fast, P. L.; Harris, M.; Truhlar, D. G. *J. Phys. Chem. A* **2000**, *104*, 4811–4815.

(60) The mPW1K functional is more accurate than B3LYP at determining the energies of nonbonding and hydrogen bonding interactions: Zhao, Y.; Truhlar, D. G. *J. Chem. Theory Comput.* **2005**, *1*, 415–432.

**Figure 12.** Calculated transition structures for the addition of HCN to acetophenone catalyzed by **1b**. Transition structures leading to the (A) major (*S*) and (B) minor (*R*) enantiomers are shown.

Consistent with experimental observations, the calculations predict that both the secondary amide and the *tert*-leucine components of the catalyst play an important role in defining enantioselectivity (entries 1–4). They also correctly identify enantioselectivity trends among related substrates using catalyst **1b** (compare entries 1, 5, and 6; 7 and 8; and 9 and 10).<sup>63,64</sup> The calculations also provide an explanation for the 60× higher reactivity of secondary amide catalysts compared with tertiary amide catalysts: in the catalyst conformation shown, a tertiary amide would block the addition of cyanide by placing an alkyl group rather than a hydrogen in the active site. Other transition structures with **1b** that avoid this have been calculated but are higher in energy ( $>0.7$  kcal/mol), presumably because the carbonyl group is pointing directly into the substrate in these conformations.

Further support for mechanism A was provided by comparison of experimental and computed isotope effects in reactions with DCN or HCN. The calculations predict an inverse HCN/DCN kinetic isotope effect of  $k_H/k_D = 0.25$  and 0.31 for the cyanation of **6a** using catalyst **1b** and **5**, respectively, consistent with the experimentally determined KIE of  $k_H/k_D \leq 0.64$  determined with catalyst **1a** (vide supra).<sup>42,65</sup>

(61) For a comparison between B3LYP and mPW1K for transition-state calculations, see: Ess, D. H.; Houk, K. N. *J. Phys. Chem. A* **2005**, *109*, 9542–9553.

(62) Examples of the use of the mPW1K functional in studying the mechanisms of complex organic reactions: (a) Cohen, R.; Rybtchinski, B.; Gandelman, M.; Rozenberg, H.; Martin, J. M. L.; Milstein, D. *J. Am. Chem. Soc.* **2003**, *125*, 6532–6546. (b) Iron, M. A.; Sundermann, A.; Martin, J. M. L. *J. Am. Chem. Soc.* **2003**, *125*, 11430–11441. (c) Fomine, S.; Tlenkopatchev, M. A. *J. Organomet. Chem.* **2006**, *691*, 5189–5196. (d) Ussing, B. R.; Hang, C.; Singleton, D. A. *J. Am. Chem. Soc.* **2006**, *128*, 7594–7607. (e) Shelton, G. R.; Hrovat, D. A.; Borden, V. T.; *J. Am. Chem. Soc.* **2007**, *129*, 164–168. (f) Henon, E.; Bercier, A.; Plantier-Royon, R.; Harakat, D.; Portella, C. *J. Org. Chem.* **2007**, *72*, 2271–2278.

(63) The calculations generally predict higher than observed selectivities for the most selective cases. For a discussion on differences between predicted and observed selectivities in catalytic asymmetric reactions, see ref 56a.

(64) In our case, mPW1K/6-31+G(d,p) is slightly more accurate than B3LYP/6-31G(d) (average absolute errors: 0.56 and 0.60 kcal/mol).

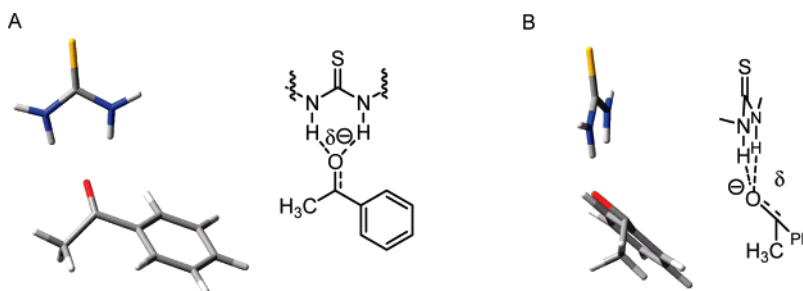


**Figure 13.** Binding geometry of the ketone–thiourea interaction in the lowest energy calculated transition state for the addition of HCN to acetophenone with catalyst **1b**: (A) front view; (B) side view.

**(1) Basis for Enantioselectivity.** The basis for high enantioselectivities in the ketone cyanation reactions can be traced to interactions of the electrophile aryl or vinyl groups with the amino acid-derived portion of the catalyst (Figure 12). As noted above, conjugated ketones have a strong preference for the  $\pi$ -system of the substrate to remain coplanar with the breaking C=O bond in the transition structure. In the pathway leading to the minor enantiomer, this geometry leads to repulsive van der Waals interactions between the substrate and the catalyst that are absent in more flexible systems such as dialkyl ketones or alanine-derived catalyst **2a**. Direct repulsive interactions between the amide  $\pi$ -system and the substrate  $\pi$ -system may be important (Table 1, entries 1 and 3).<sup>66,67</sup> The low predicted enantioselectivity for pent-3-en-2-one reacting through an *s*-trans conformation—in which the vinyl group is oriented away from the amino acid-derived portion of the catalyst—is a striking indication that high enantioselectivity is not a simple consequence of the presence of an  $sp^2$ -hybridized substituent on the ketone. Indeed, cyclohexenone, which is restricted to reacting in the *s*-trans configuration, undergoes cyanosilylation in 10% ee.

We sought to better understand the precise nature of the ketone–thiourea interaction in the cyanation reaction, and more specifically to address the question of whether one or both ketone lone pairs are engaged by the thiourea in the transition state. The computed transition structure for the dominant pathway in the cyanation of acetophenone with catalyst **1b** (Figure 12A) is reproduced in Figure 13, with all atoms except those of the thiourea unit and the ketone omitted for clarity. Inspection of this structure reveals that the partially rehybridized ketone is positioned to interact through both lone pairs in a nearly symmetrical geometry reminiscent of an enzymatic oxyanion hole.<sup>68,69</sup> This stands in sharp contrast to Lewis acid-catalyzed enantioselective additions to ketones that have been proposed to proceed through binding of a single lone pair;<sup>70–72</sup> in these cases, stereochemical induction is thought to arise from

**Table 2.** Cyanosilylation of Dialkyl Ketones Using Catalysts with Sterically Demanding Amides

entry	catalyst	ee(%) <sup>a</sup>	
		<chem>CCCCC(=O)C</chem>	<chem>c1ccccc1CC(=O)C</chem>
1	<b>1a</b>	11	8
2	<b>8</b>	54	71
3	<b>9</b>	63	84
4	<b>10</b>	65	85

<sup>a</sup> The ee values were determined by chiral GC from reactions run on 0.2 mmol scale at  $-78\text{ }^{\circ}\text{C}$  using 2.2 equiv TMSCN and 1.0 equiv  $\text{F}_3\text{CCH}_2\text{OH}$  in  $\text{CH}_2\text{Cl}_2$  (0.4 M).

the differences in Lewis basicity of the two lone pairs. The thiourea-catalyzed ketone cyanation appears to proceed through a fundamentally different mode of ketone activation that effectively involves symmetrical binding of both carbonyl lone pairs in the transition structure.

(65) KIEs were calculated from zero-point energies obtained from frequency calculations of HCN and DCN and of the transition states. The KIEs are therefore path-independent: any equilibrium isotope effects due to the formation of HCN-catalyst complexes are inconsequential.

(66) Duan, G.; Smith, V. H.; Weaver, D. F. *J. Phys. Chem. A* **2000**, *104*, 4521–4532.

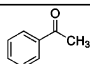
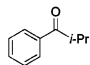
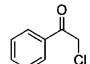
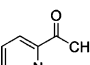
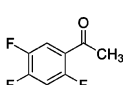
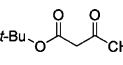
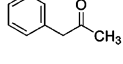
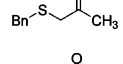
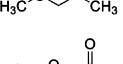
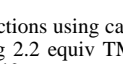
(67) This observation should be interpreted with caution, given the limitations of the B3LYP functional in describing  $\pi$ – $\pi$  interactions: Zhao, Y.; Truhlar, D. G. *Phys. Chem. Chem. Phys.* **2005**, *2701*–2705. Efforts to probe this interaction using electronically differentiated substrates were inconclusive. We observe sharp decreases in enantioselectivity when using electron-deficient acetophenone derivatives. However, these more reactive substrates may react via an entirely different, less selective mechanism.

(68) A detailed analysis of the geometry of thiourea–ketone interactions with all ten catalyst–substrate combinations listed in Table 1 is provided in the Supporting Information.

(69) Theoretical analyses of transition structures for the enzymatic additions to carbonyl groups involving hydrogen bonding: (a) Wlodek, S. T.; Antosiewicz, J.; Briggs, J. M. *J. Am. Chem. Soc.* **1997**, *119*, 8159–8165. (b) Li, G.-S.; Maigret, B.; Rinaldi, D.; Ruiz-López, M. F. *J. Comput. Chem.* **1998**, *19*, 1675–1688. (c) Nishihara, J.; Tachikawa, H. *J. Theor. Biol.* **1999**, *196*, 513–519. (d) Zhang, Y.; Kua, J.; McCammon, J. A. *J. Am. Chem. Soc.* **2002**, *124*, 10572–10577. (e) Zhan, C.-G.; Zheng, F.; Landry, D. W. *J. Am. Chem. Soc.* **2003**, *125*, 2464–2474. (f) Tachikawa, H.; Igarishi, M.; Nishihara, J.; Ishabishi, T. *J. Photochem. Photobiol. B* **2005**, *79*, 11–23. (g) Gao, D.; Zhan, C.-G. *J. Phys. Chem. B* **2005**, *109*, 23070–23076. (h) Manojkumar, T. K.; Cui, C.; Kim, K. S. *J. Comput. Chem.* **2005**, *26*, 606–611.

(70) For examples, see: (a) Corey, E. J.; Helal, C. J. *Tetrahedron Lett.* **1995**, *36*, 9153–9156. (b) Noyori, R.; Hashiguchi, S. *Acc. Chem. Res.* **1997**, *30*, 97–102. (c) Corey, E. J.; Helal, C. J. *Angew. Chem., Int. Ed.* **1998**, *37*, 1986–2012. (d) Masumoto, S.; Suzuki, M.; Kanai, M.; Shibasaki, M. *Tetrahedron* **2004**, *60*, 10497–10504. (e) Kim, J. G.; Waltz, K. M.; Garcia, I. F.; Kwiatkowski, D.; Walsh, P. J. *J. Am. Chem. Soc.* **2004**, *126*, 12580–12585. For a crystal structure of an aldehyde bound to a chiral Lewis acid, see: (f) Huang, F.; Iwama, T.; Rawal, V. H. *J. Am. Chem. Soc.* **2002**, *124*, 5950–5951.

**Table 3.** Enantioselective Cyanosilylation of Ketones Promoted by Optimized Catalysts **8** and **10**

$  \begin{array}{c} \text{O} \\ \parallel \\ \text{R}-\text{C}-\text{R}' \end{array} + \text{TMSCN} \xrightarrow[\text{catalyst (5 mol\%), -78 }^\circ\text{C}]{\text{CF}_3\text{CH}_2\text{OH, CH}_2\text{Cl}_2/\text{toluene}} \begin{array}{c} \text{O} \quad \text{CN} \\ \parallel \quad \diagup \\ \text{R}-\text{C}-\text{R}' \end{array}  $						
entry	ketone	catalyst <sup>a</sup>	time (h)	yield <sup>b</sup> (%)	ee <sup>c</sup> (%)	ee <sup>c</sup> with <b>1a</b> (%)
1		<b>8</b>	36	88	98	97
2		<b>8</b>	60	91	95	86
3		<b>8</b>	12	98	92	89
4		<b>8</b>	12	97	96	94
5		<b>8</b>	12	90	90	78
6		<b>10</b>	18	98	92	59
7		<b>10</b>	18	95	85	8
8 <sup>d</sup>		<b>10</b>	12	96	84	51
9 <sup>d</sup>		<b>10</b>	8	81	88	79
10 <sup>d</sup>		<b>10</b>	8	91	86	60

<sup>a</sup> Reactions using catalyst **8** were run on 1.0 mmol scale in CH<sub>2</sub>Cl<sub>2</sub> (0.5 M) using 2.2 equiv TMSCN and 1.0 equiv CF<sub>3</sub>CH<sub>2</sub>OH. Reactions using catalyst **10** were run on 1.0 mmol scale in 3:1 CH<sub>2</sub>Cl<sub>2</sub>/toluene (0.4 M).

<sup>b</sup> Isolated yields after silica gel chromatography. <sup>c</sup> Determined by chiral GC.

<sup>d</sup> Reaction run using 2.5 mol % catalyst.

**D. Development of More Highly Enantioselective Catalysts.** Catalyst **1a** promotes the cyanosilylation of dialkyl ketones with low enantioselectivity (Table 2, entry 1), and high ee's are observed only with aryl-alkyl or alkenyl-alkyl ketones. However, the computational studies described above suggest that the basis for high enantioinduction results from direct steric and electronic interactions of the substrate with the amino acid-derived portion of the catalyst. On this basis, we reasoned that improved results in the asymmetric cyanosilylation of ketones may be obtained by accentuating these interactions; in particular, fine-tuning the steric properties of the amide could potentially lead to catalysts that promote the highly enantioselective cyanosilylation of dialkyl ketones.

In accord with this hypothesis, analogues of **1a** bearing more sterically demanding secondary amides yielded addition products in substantially higher ee's (Table 2, entries 2–4). Catalyst **8**

proved to be the most selective cyanosilylation catalyst for acetophenone reported to date (Table 3, entry 1); in addition highly electron-deficient and sterically demanding aromatic ketones—challenging substrates with the first generation catalyst—undergo cyanosilylation to provide silylcyanohydrins in excellent yield and enantiomeric excess (entries 2–5). The more sterically demanding catalyst **10** proved effective at catalyzing the cyanosilylation of a range of dialkyl ketones in excellent yields and useful levels of enantiomeric excess (entries 6–10). The fact that 2-heptanone undergoes cyanosilylation in lower enantiomeric excess than dialkyl ketones bearing  $\pi$  or lone pair substituents is consistent with our hypothesis that direct electronic interactions between substrate and catalyst play an important role in controlling enantioinduction.

## Conclusions

A wide range of experimental and theoretical results support the proposal that the amino-thiourea catalyzed ketone cyanosilylation proceeds through a mechanism that involves simultaneous activation of HCN by the tertiary amine and of the ketone by the thiourea. Key experiments and findings include the following:

(1) Kinetic analysis under synthetically relevant conditions is consistent with ternary transition structure **1a**•HCN•**6b** and revealed mechanistically significant inhibition effects at elevated concentrations.

(2) Kinetic analysis in the presence of inactive inhibitors and isotopically substituted substrates provides strong evidence that both the thiourea and tertiary amine are involved directly in catalysis.

(3) <sup>1</sup>H NMR experiments using substrates with different steric properties were used to distinguish between medium effects and thiourea binding, providing a potentially general method for characterizing these interactions.

(4) Transition state DFT calculations reproduce experimental trends in enantioselectivity across a range of substrates and catalysts, thereby providing strong evidence for a mechanism of catalysis involving ketone–thiourea rather than cyanide–thiourea interactions.

(5) Analysis of the transition structures reveals a basis for enantioselectivity that involves direct substrate–catalyst interactions and binding through both ketone lone pairs, suggesting that the mode of asymmetric induction with chiral hydrogen-bond donors may be fundamentally different than with chiral Lewis acids.

The recent emergence of a wide variety of catalytic asymmetric reactions that are proposed to operate via cooperative mechanisms suggests that cooperative reactivity may play as dominant a role in small-molecule asymmetric catalysis as it does in enzymatic catalysis. However, even when structure–activity relationships indicate that multiple functional groups are necessary for catalysis, several different mechanisms are often possible, and these mechanistic possibilities are often difficult to distinguish. The present study represents a case in which it has been possible to fully characterize the rate- and selectivity-determining step of a synthetically interesting reaction promoted by a bifunctional catalyst, and it highlights how classical and modern mechanistic tools can be used successfully in combination to probe complex transition structures in asymmetric catalysis. This work has provided necessary insight

- (71) For discussions and leading references on carbonyl binding to hydrogen-bond donors, see: (a) Etter, M. C. *Acc. Chem. Res.* **1990**, *23*, 120–126. (b) Phiko, P. M. *Angew. Chem., Int. Ed.* **2004**, *43*, 2062–2064. See, also ref 16d.
- (72) For an example of a hydrogen-bond donor proposed to activate carbonyls by binding through a single lone pair, see: (a) Unni, A. K.; Takenaka, N.; Yamamoto, H.; Rawal, V. H. *J. Am. Chem. Soc.* **2005**, *127*, 1336–1337. (b) Gordillo, R.; Dudding, T.; Anderson, C. D.; Houk, K. N. *Org. Lett.* **2007**, *9*, 501–503 and refs cited therein.



into one class of thiourea-catalyzed reactions, and we expect that many of the results may be generally applicable. Nevertheless, it would be premature to conclude that all thiourea-catalyzed reactions proceed via analogous mechanisms: we remain intrigued and often perplexed by the mechanistic possibilities that other thiourea-catalyzed reactions suggest. The current work indicates that characterizing this potential mechanistic diversity may be possible.

**Acknowledgment.** This work was supported by the NIH (GM-43214). We thank Prof. Charles B. Musgrave (Stanford),

Dr. Lars P. C. Nielsen, and a referee for helpful suggestions, and Ye Tao for assistance in the preparation of several catalysts.

**Supporting Information Available:** Complete ref 50; complete experimental procedures, characterization data, chiral chromatographic analyses of racemic and enantiomerically enriched products, kinetic data, derivation of eq 2,  $^1\text{H}$  NMR titration data, and geometries and energies of calculated stationary points. This material is available free of charge via the Internet at <http://pubs.acs.org>.

JA0735352